International Journal of Infrared and Millimeter Waves, Vol. 14, No. 8, 1993

FAR-INFRARED SELF-BROADENING AND PRESSURE SHIFT MEASUREMENTS OF METHYL CYANIDE

G. W. Schwaab, K. M. Evenson, and L. R. Zink

Max-Plank-Institut für Radioastronomie
auf dem Hügel 69,
D-5300 Bonn
National Institute of Standards and Technology
325 Broadway
Boulder, Colorado 80303

Received May 25, 1993

Abstract

Pressure shifts and self-broadening parameters of the J=43←42, J=44←43, J=56←55 and J=68←67 sub-bands of the $^1A_1$ ground state of $CH_3C^{14}N$ up to K=10 were determined using the NIST tunable far-infrared (TuFIR) spectrometer . The pressure shift agrees well with theoretical predictions made using Anderson-Tsao-Curnutte theory. The self-broadening parameter shows the expected K depencence. However, the predictions are systematically too large for decreasing J. The influence of the TuFIR power spectrum on the derived experimental parameters was evaluated and a comparison was made between two-wave and three-wave mixing spectroscopy.

keywords: far-infrared spectrometer, methyl cyanide, pressure broadening, pressure shift

1 Introduction

Pressure shift and self-broadening parameters in the microwave to infrared spectral regions are usually described by impact theories (1, 2, 3, 4). These theories assume a complete loss of coherence of the emitted radiation for close collisions and use a classical path approximation to take account of the long-range intermolecular interactions. They differ mainly in their assumptions for the intermediate range interaction.

In the theory of Anderson, Tsao, and Curnutte (ATC-theory) (1, 4), the probability function which describes the efficiency of collisions due to long-range forces is extrapolated to a minimum collision parameter b_0 where the

0195-9271/93/0800-1643$07.00/0

probability of disturbing the radiation process equals 1. Thus, the overall cross section σ can be represented as the sum of a hard sphere cross section $\sigma_{inner} = \pi b_0^2$, where b_0 is the radius of the molecule, and an outer part σ_{outer}, which depends on the type of long range intermolecular interaction.

To compare the theoretical predictions of ATC-theory with experimental data, methyl cyanide was chosen. Its large dipole moment (3.93 D) makes the dipole-dipole interaction the dominant source of self-broadening and pressure shift. The resulting b_0 is in the range of 1-2 nm so that the classical path assumption is well justified.

Pressure broadening and pressure shift measurements on the isotopic species $CH_3C^{14}N$ and $CH_3C^{15}N$ have been reported by several authors (5, and references therein) involving energy levels up to J=6. The experimental data usually agree within to 30% with values predicted by ATC-theory. Unfortunately, accurate determination of self-broadening and pressure shift parameters for $CH_3C^{14}N$ is complicated at low J by hyperfine splitting. This can be overcome by observing higher-J rotational transitions. Recently self-broadening parameter studies at higher-J levels have also been reported (6). In order to extend the available data well into the submillimeter range we used a tunable far-infrared (TuFIR) source to measure self-broadening and shift parameters of ground state rotational transitions of $CH_3C^{14}N$ involving levels up to J=68. In this paper we place emphases on the K dependency and on the limitations of the spectroscopic method; the J-dependency has been discussed more completely elsewhere (7).

2 Experimental Details

2.1 The TuFIR Spectrometer

We used the TuFIR spectrometer at the National Institute of Standards and Technology (NIST) in Boulder, Colorado, to produce coherent FIR radiation (8). The system can be operated in two ways. In second-order operation (see Fig. 1) two CO_2 laser frequencies are mixed in a metal-insulator-metal (MIM) diode to produce a difference frequency in the FIR. In order to have tunability together with very high frequency accuracy, the first laser is saturated-absorption-stabilized, and the second laser is a high-pressure waveguide laser which is referred to a second absorption-stabilized fixed-frequency CO_2 laser. Each laser frequency can be shifted by plus or minus 90 MHz by the two acousto-optic modulators. Thus, the overall frequency coverage of one pair of laser differences is of the order of 560 MHz ($\pm$180 MHz from the acousto-optic modulators and $\pm$100 MHz tunability of the high pressure CO_2 laser). The uncertainty of the radiated FIR fre-

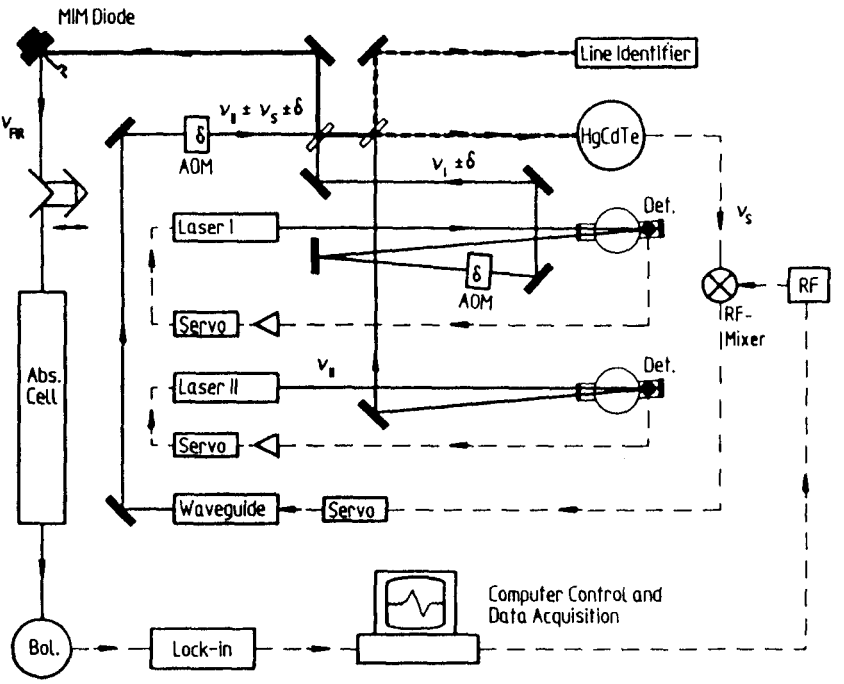

Figure 1: TuFIR spectrometer in second-order operation: two CO_2 lasers (*Laser I* and *Waveguide*) are mixed in a MIM diode to produce the difference frequency $\nu_{FIR} = |(\nu_I \pm \delta) \pm (\nu_{II} \pm \nu_S \pm \delta)|$. *Laser I* is saturated-absorption stabilized. The waveguide laser is referred to the stabilized *Laser II* by the frequency difference produced in the HgCdTe detector. Both laser frequencies can be shifted by 90 MHz by acousto-optic modulators (*AOM*). The FIR radiation is detected by a liquid helium cooled bolometer. The data acquisition is fully computerized.

quency is given by the quadrature sum of the uncertainties of the saturated absorption stabilized CO_2 lasers which amounts typically to 10 kHz (9).

To obtain more tunability, third-order operation is used (see Fig. 2): two stabilized CO_2 lasers with frequencies ν_I and ν_{II} are mixed with microwave radiation ν_μ (5 to 20 GHz) in a MIM diode to produce upper and lower sideband radiation at the difference frequency:

$$\nu_{FIR} = |\nu_I - \nu_{II}| \pm \nu_\mu. \tag{1}$$

The drawbacks of this method compared to second-order operation are lower power, higher relative noise, and — especially for more complex

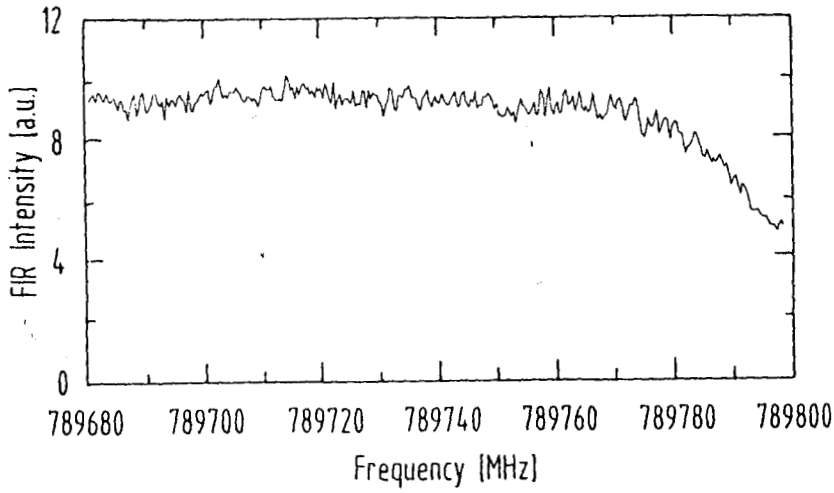

Figure 3: FIR power versus frequency for second order operation

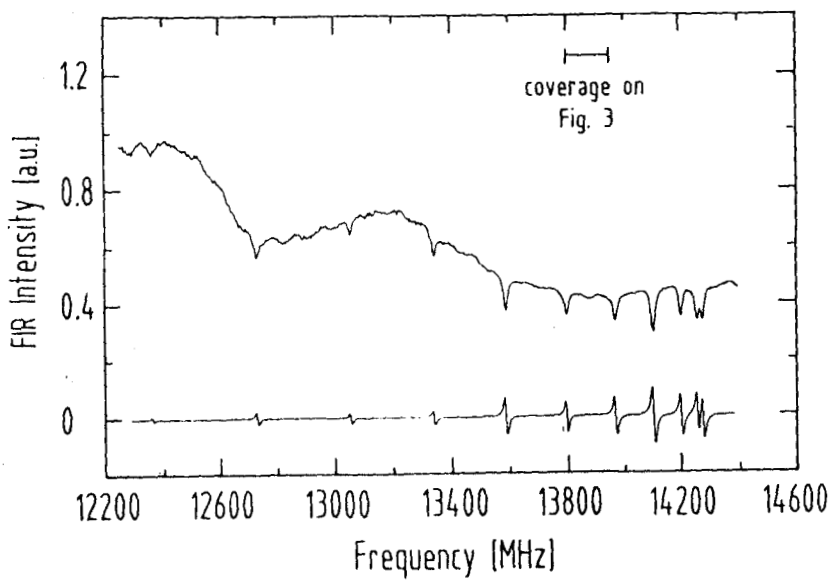

Figure 4: Comparison of AM (upper trace) and FM (lower trace) spectrum for the J=56←55 multiplet of methyl cyanide. The abscissa shows the frequency of the microwave source.

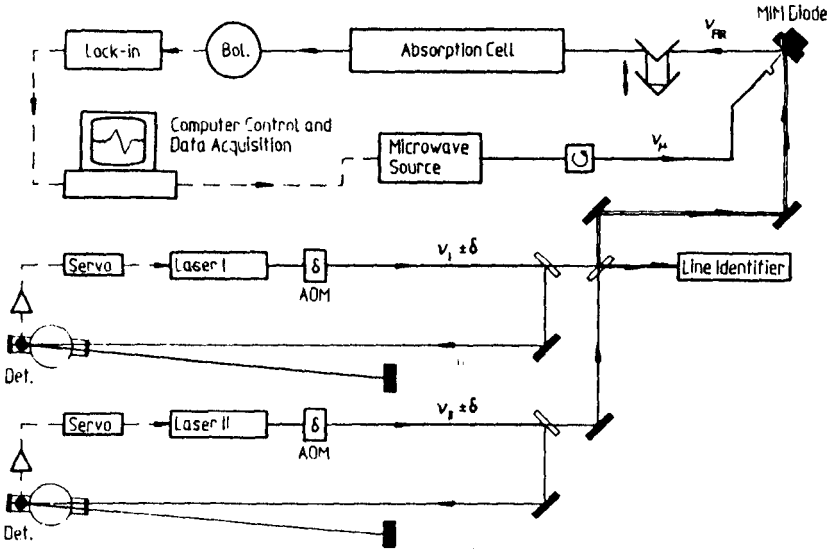

Figure 2: TuFIR spectrometer in third-order operation: two frequency stabilized CO_2 lasers (*Laser I* and *Laser II*) are mixed with a microwave component in a MIM diode to produce the frequencies $\nu_{FIR} = |\nu_I - \nu_{II}| \pm \nu_\mu$

Table I: CO_2 laser lines and frequencies (10) which were used for the determination of the self-broadening parameters of CH_3CN

trans J K	ord	Laser I line	Laser I frequ. [MHz]	Laser II line	Laser II frequ. [MHz]	$\lvert\nu_{II} - \nu_I\rvert$ [MHz]
42 0,1,3	2	$^{13}C^{16}O_2$ 9P(14)	30 160 719.906	$^{12}C^{16}O_2$ 10R(26)	29 370 829.621	789 890.285
42 6	2	$^{13}C^{16}O_2$ 10P(18)	26 940 814.241	$^{12}C^{16}O_2$ 10P(40)	27 730 022.416	789 208.175
42 0-9	3	$^{13}C^{16}O_2$ 9P(26)	29 828 925.529	$^{12}C^{16}O_2$ 10R(10)	29 054 072.700	774 852.829
43 0-9	3	$^{13}C^{16}O_2$ 9P(14)	30 160 719.906	$^{12}C^{16}O_2$ 9P(34)	30 983 190.757	822 470.850
55 0-10	3	$^{13}C^{16}O_2$ 9P(36)	29 529 351.466	$^{12}C^{16}O_2$ 10P(12)	28 516 026.658	1 013 324.809
67 0-9	3	$^{13}C^{16}O_2$ 9P(34)	29 590 913.428	$^{12}C^{16}O_2$ 10P(18)	28 359 773.810	1 231 139.619

molecules — blending of lines in the image sideband with lines in the signal sideband.

Since the ground state rotational transitions of methyl cyanide are strong, its self-broadening parameters are large and a K-multiplet typically covers a region of a few gigahertz, we used the third-order system for nearly all measurements. For comparison, we measured the J=42, K=0, 1, 3, 6 transitions in both second- and third-order operation. A list of the CO_2 laser pairs used for the measurements in this paper is given in Table I.

The MIM contacts consisted of an electrochemically pointed, 25 μm diameter tungsten wire contacting a polished Ni (second-order operation)

or Co (third-order operation) substrate at normal incidence. A corner reflector was adjusted to improve the FIR radiation pattern. The beam was reflected by an off-axis parabola and sent through a single-pass absorption cell consisting of a pyrex tube of 22 mm inner diameter and high-density polyethylene windows. Cells with lengths from 3 to 84 cm were used depending on the different line strengths.

To reduce standing waves, all optical components were slightly tilted or wedged, and the optical path length was modulated by several wavelengths with a moving mirror system. The radiation was detected by a pumped (2 K) liquid-He-cooled, Ga-doped Ge bolometer with a NEP of 10^{-13} W/$\sqrt{Hz}$. FIR powers of 10 to some 100 nW were obtained using 300 mW CO_2 laser power and 3–8 mW of microwave power. A minimum detectable absorptivity of 10^{-6} cm^{-1} in a 1 m absorption cell was realized. The FIR frequency was modulated at a rate of 1 kHz with an amplitude of 0.8 MHz. During the measurements the temperature varied from 302 to 304 K. Pressures ranged from 0.05–0.6 Torr and were measured with an accuracy of 3% with temperature stabilized precision capacitance manometers; 6–10 data pairs were used to evaluate the broadening and shift parameters of each line. We flowed the gas slowly to maintain the pressure and to compensate for absorption of methyl cyanide on the walls of the cell.

To estimate the influence of power variations on the linewidths we obtained power spectra for both methods of operation. In the second-order case (see Fig. 3), the laser can be tuned ±100 MHz, and its 90% power point is ±60 MHz on most of the CO_2 lines. For third-order operation (see Fig. 4) the power spectrum is nearly constant on a single line, but varies from line to line due to standing waves in the microwave coaxial line connecting the synthesizer to the MIM diode. However, this variation is not exhibited in the derivative spectrum, because the FIR frequency modulation is a result of modulating the frequency of one of the CO_2 lasers on top of its gain curve. The center frequencies can be determined in third-order operation as accurately as in second-order operation. However, the FIR power variation may produce some systematic errors to the measured linewidths and the pressure broadening parameters derived from them depending on the ratio of the linewidths to the period of the standing waves.

2.2 Data Analysis

The data were analyzed using a nonlinear least squares fitting routine provided by Chance (11). The program fits Voigt profiles to directly measured or frequency-modulated spectra. The heart of the fitting routine is the Levenberg-Marquardt, nonlinear-least-squares technique described in (12).

To save computing time, the Voigt profile was approximated with an appropriate formula. Comparison of the approximation with tabulated values (13) for small Lorentzian/Gaussian width ratios yields maximum errors of less than 2 percent for a single spectral point. At larger ratios the error drops well below 1 percent. The partial derivatives of the Voigt profile were directly calculated as differentials. In addition, frequency-modulated spectra were fitted using a six-point, derivative modulation scheme. The effects of line saturation were included in the fits. Fitting parameters for each spectrum were the baseline offset, a multiplicative scaling factor, and for each line, the Lorentzian width and the center frequency. The half 1/e Gaussian half-width Γ_G and the line intensities were kept constant at their theoretical values.

The spectra of the K=4-transitions of the multiplets J=43←42, J=44←43, J=56←55 and J=68←67 at a pressure of 200 mTorr are shown in Fig. 5 together with the corresponding fits and the resulting residuals. The frequencies given on the abscissa of each plot are those of the microwave source. The signal-to-noise ratio varied with the lengths of the absorption cells and the FIR-intensity, and was in the range from 20 to 100. For the J=56←55 and J=68←67 measurements, the S/N was sufficient to permit the observation of the difference between the approximate Voigt profile and its real counterpart.

3 Results

The experimentally obtained pressure shifts s and self-broadening parameters Γ of methyl cyanide are given in Table II. Figure 6 shows the K dependency of the self-broadening parameter for the different J transitions. For each transition s and Γ were determined by least square fitting. An example is shown in Fig. 7. Since the center frequencies could be determined very accurately even for slightly blended lines they were weighted by $1/\sigma^2$ to obtain s. The zero-pressure center frequencies are not listed in Table II. They will be published in a forthcoming paper together with line frequencies of vibrationally excited CH_3CN. The self-broadening parameters were obtained using unweighted least square fitting. Here, systematic errors due to frequency dependent FIR power variations, overlapping lines and base line variations are difficult to take into account.

The frequency shift is negative for all measured transitions. It is constant within each K multiplet. The weighted averages are -1.13(11) MHz/Torr, -1.02(13) MHz/Torr, -0.80(7) MHz/Torr and -0.51(6) MHz/Torr for the J=43←42, J=44←43, J=56←55 and J=68←67 multiplet, respectively.

Like the pressure shift, the self-broadening parameter of methyl cyanide

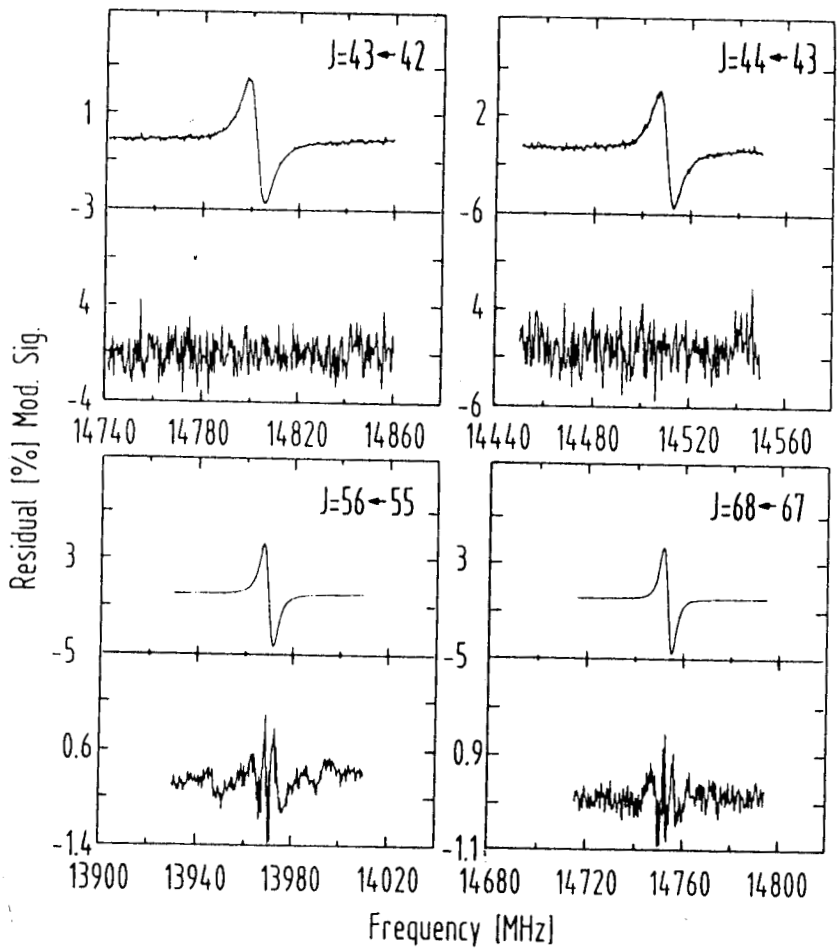

Figure 5: Spectra of the K=4 rotational transitions of the CH_3CN ground state with their corresponding fits and the resulting residuals. The abscissa shows the frequency of the microwave source. The difference in the S/N ratios is due to the variation in FIR power.

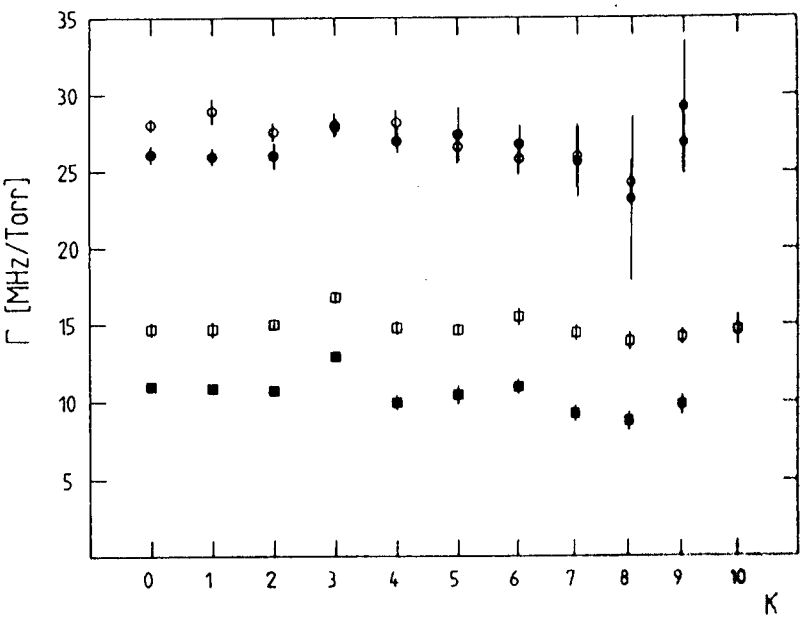

Figure 6: K dependency of the self-broadening parameter Γ of the J=43←42 (○), J=44←43 (●), J=56←55 (□) and J=68←67 (■) multiplets. The error bars represent a 3σ deviation

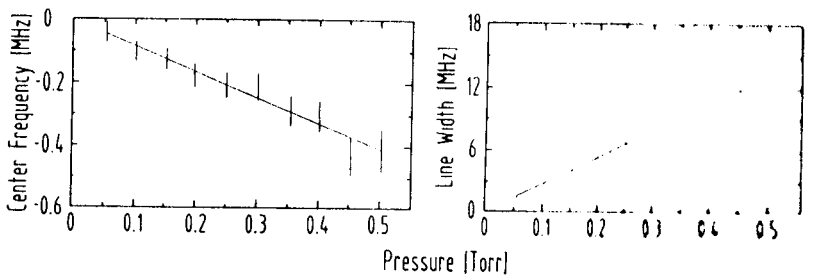

Figure 7: Pressure shift (left, with 3σ-error bars) and self broadening (right) of the J=43←42, K=6 transition of CH_3CN

Table II: Pressure shifts and self-broadening parameters of selected ground state rotational transitions of CH_3CN. The theoretical predictions include dipole-dipole, dipole-quadrupole and quadrupole-quadrupole interactions (14)

J K	s[a] [MHz/Torr] exp	theor	Γ[a] [MHz/Torr] exp	theor	J K	s[a] [MHz/Torr] exp	theor	Γ[a] [MHz/Torr] exp	theor
42 0	-0.69 (32)	-1.14	28.04 (39)	42.09	55 0	-0.63(23)	-0.86	14.69 (42)	18.85
42 1	-1.46 (34)	-1.14	28.93 (80)	42.08	55 1	-1.00(23)	-0.86	14.69 (48)	18.85
42 2	-1.21 (31)	-1.13	27.58 (55)	42.07	55 2	-0.82(23)	-0.86	15.01 (11)	18.85
42 3	-1.23 (27)	-1.12	28.04 (72)	42.05	55 3	-0.85(27)	-0.85	16.80 (34)	18.85
42 4	-1.19 (33)	-1.11	28.20 (75)	42.02	55 4	-0.97(23)	-0.84	14.79 (40)	18.85
42 5	-1.39 (36)	-1.09	26.63(106)	41.98	55 5	-0.85(23)	-0.84	14.66 (35)	18.85
42 6	-0.82 (32)	-1.07	25.83(100)	41.93	55 6	-0.70(23)	-0.82	15.52 (54)	18.85
42 7	-0.90 (60)	-1.05	26.05(203)	41.88	55 7	-0.76(24)	-0.81	14.48 (47)	18.85
42 8	-1.45 (72)	-1.02	24.30(141)	41.82	55 8	-0.67(25)	-0.78	13.94 (57)	18.85
42 9	-1.15 (71)	-0.98	26.90(188)	41.75	55 9	-0.81(23)	-0.77	14.21 (56)	18.85
43 0	-0.94 (35)	-1.13	26.38 (60)	39.62	55 10	-0.65(31)	-0.75	14.68(101)	18.85
43 1	-1.14 (36)	-1.12	26.30 (53)	39.61	67 0	-0.39(18)	-0.59	11.00 (24)	10.27
43 2	-1.09 (35)	-1.12	26.31(102)	39.60	67 1	-0.66(18)	-0.59	10.89 (19)	10.27
43 3	-0.96 (30)	-1.11	27.90 (55)	39.58	67 2	-0.65(18)	-0.59	10.76 (18)	10.27
43 4	-1.07 (41)	-1.10	27.00 (74)	39.56	67 3	-0.48(20)	-0.59	12.96 (32)	10.27
43 5	-1.30 (47)	-1.08	27.43(172)	39.53	67 4	-0.52(19)	-0.58	9.97 (46)	10.27
43 6	-0.79 (35)	-1.06	26.82(118)	39.49	67 5	-0.41(21)	-0.57	10.49 (58)	10.27
43 7	-1.46 (76)	-1.04	25.65(226)	39.44	67 6	-0.60(20)	-0.56	11.01 (46)	10.27
43 8	-0.85 (94)	-1.01	23.23(531)	39.39	67 7	-0.33(21)	-0.55	9.26 (51)	10.27
43 9	-0.51(128)	-0.98	29.22(444)	39.33	67 8	-0.55(22)	-0.54	8.78 (58)	10.28
					67 9	-0.50(28)	-0.53	9.85 (69)	10.28

[a] numbers in parentheses give the 3σ deviations in units of the last digit

decreases with increasing J. It drops from 27.6(11) MHz/Torr for J=43←42 to 10.5(11) MHz/Torr for J=68←67. A more detailed analysis of the J dependence of s and Γ is given in (7) together with further data obtained with a similar instrument. In contrast with the the lower-J measurements, the J=56←55 and J=68←67 multiplets self-broadening parameters of the K=3n, n=1, 2, 3 lines are significantly larger than those with $K \neq 3n$. This is probably due to saturation effects and leads to an estimation of 2 MHz/Torr for the systematic errors of the strong lines.

A comparison of second- and third-order spectroscopy is shown in Table III for the transitions J=43←42, K=0, 1, 3, 6. The results agree within their 3σ-error bars for all transitions. While the center frequencies can be derived with equal accuracy by each method, the small frequency range which can be covered by second-order spectroscopy leads to large errors in Γ and s – especially for the closely spaced transitions K=0 and 1. For these transitions, pressures of 200 mTorr produced systematic errors due to the merging of both lines. In addition, the baseline is difficult to define and

Table III: Comparison of second- and third-order operation of the MIM spectrometer

J K	second-order operation			third-order operation		
	ν_0[a] [MHz]	s[a]	Γ[a] [MHz/Torr]	ν_0[a] [MHz]	s[a]	Γ[a] [MHz/Torr]
42 0	789 894.270 (81)	-0.93(74)	28.68 (794)	789 894.183(81)	-0.69(32)	28.04 (39)
42 1	789 879.329 (80)	-0.81(70)	33.20(1311)	789 879.347(82)	-1.46(34)	28.93 (80)
42 3	789 759.854 (86)	-1.10(32)	30.62 (158)	789 759.827(73)	-1.23(27)	28.04 (72)
42 6	789 357.043(112)	-1.29(70)	26.28 (126)	789 357.098(81)	-0.82(32)	25.83(100)

[a] numbers in parentheses give the 3 σ deviations in units of the last digit

the K=2 line starts to appear. The agreement gets better for K=3. Here, systematic errors occur for pressures above 400 mTorr. Because of the large self-broadening the entire line width can then not be covered completely for high pressures. Fitting of these data leads to line widths which are systematically too large. For molecules with large self-broadening parameters and a dense spectrum, second-order spectroscopy is of only very limited use for the determination of broadening and shift parameters.

4 Conclusions

As Tables II and III show, the TuFIR spectrometer represents a very powerful tool for determining pressure shifts and broadening parameters of molecular species in the far infrared. Its limited frequency range in second-order operation makes third-order spectroscopy the preferable choice for measuring molecules with closely spaced lines and large broadening coefficients. Second-order spectroscopy lead to systematic errors in the present work.

As Table II shows, the experimentally derived pressure shifts and self-broadening parameters compare well with theoretical predictions by ATC-theory. The J levels observed here lie above the most populated states. They are therefore above the self-broadening maximum induced by the absorber-perturber resonance described in (7) and show the expected rapidly decreasing Γ with increasing J. However, ATC-theory overestimates the magnitude of the increase of Γ with decreasing J. For $K \ll J$ no K dependence of the self-broadening parameter is predicted and a statistically insignificant decrease for J=43←42 and J=44←43 was measured. The pressure shifts are within their error bars in full agreement with the theoretical predictions.

There are two ways to improve the accuracy of the derived parameters.

An improved S/N ratio would justify the use of a fully calculated Voigt profile instead of an approximated one and the derivative spectra could be normalized with the FIR power. This would reduce the systematic errors and accurately test the FIR line shapes.

We thank G.Buffa and O.Tarrini for the calculation of the theoretically predicted pressure shifts and self-broadening parameters and their helpful discussions.

References

(1) P. W. Anderson, "Pressure Broadening in the Microwave and Infra-Red Regions", Phys. Rev. **76**, 647-661 (1949)

(2) R. P. Leavitt, D. Korff, "Cutoff-Free Theory of Impact Broadening and Shifting in Microwave and Infrared Gas Spectra", J. Chem. Phys. **74**, 2180-2188 (1981)

(3) J. S. Murphy, J. E. Boggs, "Collision Broadening of Rotational Absorption Lines. I. Theoretical Formulation", J. Chem. Phys. **47**, 691-702 (1967)

(4) C. J. Tsao, B. Curnutte, "Line-Widths of Pressure-Broadened Spectral Lines", J. Quant. Spectrosc. Radiat. Transfer **2**, 41-91 (1962)

(5) G. Buffa, D. Giulietti, M. Lucchesi, M. Martinelli, O. Tarrini, "Collisional Line Shape for the Rotational Spectrum of Methylcyanide: Experiments and Theory", J. Chem. Phys. **90**, 6881-6886 (1989)

(6) G. W. Schwaab, D. Galleguillos, R. Wattenbach, H. P. Röser, "Heterodyne Spectroscopy of Rotational Transitions in PH_3, CH_3CN, and H_2CO at 800 GHz", Proc. of the Fourth International Conference on Infrared Physics held from Aug. 22-26 in Zürich, Switzerland (editors: R. Kesselring, F. K. Kneubühl), 513-515 (1988)

(7) G. Buffa, O. Tarrini, P.De Natale, M. Inguscio, F. S. Pavone, M. Prevedelli, K. M. Evenson, L. R. Zink, G. W. Schwaab, "Evidence of Absorber-Perturber Resonance in the Self-Broadening of the Methyl Cyanide FIR spectrum, Phys. Rev. A , 6443-6450 (1992)

(8) K. M. Evenson, D. A. Jennings, M. D. Vanek, "Tunable Far-Infrared Laser Spectroscopy", in *Frontiers of Laser Spectroscopy of Gases*, A. C. P. Alves, J. M. Brown, J. M. Hollas (edts.), pp. 43-51, Kluwer Academic Publishers, Dordrecht 1988

(9) T. D. Varberg, K. M. Evenson, "Accurate Far-Infrared Rotational Frequencies of Carbon Monoxide", Ap. J. **385**, 763–765 (1992)

(10) F. R. Petersen, E. C. Beatty, C. R. Pollock, "Improved Rovibrational Constants and Frequency Tables for the Normal Laser Bands of $^{12}C^{16}O_2$", J. Mol. Spectr. **102**, 112–122 (1983)

(11) K. V. Chance, Harvard Smithsonian Center for Astrophysics, private communication (1989)

(12) W. H. Press, B. Flannery, S. A. Teukolski, W. T. Vetterling, *Numerical Recipes*, Chapter 14, published by Press Syndicate of the University of Cambridge, Cambridge,MA (1988)

(13) D. W. Posener, "The Shape of Spectral Lines: Tables of the Voigt Profile", Austr. J. Phys. **12**, 184–196 (1959)

(14) G. Buffa, O. Tarrini, Dipartimento di Fisica dell' Università di Pisa, private communication (1990)